SARS-CoV replication and pathogenesis in an *in vitro* model of the human conducting airway epithelium

Amy C. Sims [a,*], Susan E. Burkett [c], Boyd Yount [a], Raymond J. Pickles [b,c]

[a] *Department of Epidemiology, University of North Carolina at Chapel Hill, Chapel Hill, NC 27599, United States*
[b] *Department of Microbiology and Immunology, University of North Carolina at Chapel Hill, Chapel Hill, NC 27599, United States*
[c] *The Cystic Fibrosis Center, University of North Carolina at Chapel Hill, Chapel Hill, NC 27599, United States*

Available online 23 April 2007

Abstract

SARS coronavirus (SARS-CoV) emerged in 2002 as an important cause of severe lower respiratory tract infection in humans and *in vitro* models of the lung are needed to elucidate cellular targets and the consequences of viral infection. The severe and sudden onset of symptoms, resulting in an atypical pneumonia with dry cough and persistent high fever in cases of severe acute respiratory virus brought to light the importance of coronaviruses as potentially lethal human pathogens and the identification of several zoonotic reservoirs has made the reemergence of new strains and future epidemics all the more possible. In this chapter, we describe the pathology of SARS-CoV infection in humans and explore the use of two models of the human conducting airway to develop a better understanding of the replication and pathogenesis of SARS-CoV in relevant *in vitro* systems. The first culture model is a human bronchial epithelial cell line Calu-3 that can be inoculated by viruses either as a non-polarized monolayer of cells or polarized cells with tight junctions and microvilli. The second model system, derived from primary cells isolated from human airway epithelium and grown on Transwells, form a pseudostratified mucociliary epithelium that recapitulates the morphological and physiological features of the human conducting airway *in vivo*. Experimental results using these lung epithelial cell models demonstrate that in contrast to the pathology reported in late stage cases SARS-CoV replicates to high titers in epithelial cells of the conducting airway. The SARS-CoV receptor, human angiotensin 1 converting enzyme 2 (hACE2), was detected exclusively on the apical surface of cells in polarized Calu-3 cells and human airway epithelial cultures (HAE), indicating that hACE2 was accessible by SARS-CoV after lumenal airway delivery. Furthermore, in HAE, hACE2 was exclusively localized to ciliated airway epithelial cells. In support of the hACE2 localization data, the most productive route of inoculation and progeny virion egress in both polarized Calu-3 and ciliated cells of HAE was the apical surface suggesting mechanisms to release large quantities of virus into the lumen of the human lung. Preincubation of the apical surface of cultures with antisera directed against hACE2 reduced viral titers by two logs while antisera against DC-SIGN/DC-SIGNR did not reduce viral replication levels suggesting that hACE2 is the primary receptor for entry of SARS-CoV into the ciliated cells of HAE cultures. To assess infectivity in ciliated airway cultures derived from susceptible animal species we generated a recombinant SARS-CoV by deletion of open reading frame 7a/7b (ORF 7a/7b) and insertion of the green fluorescent protein (GFP) resulting in SARS-CoV GFP. SARS-CoV GFP replicated to similar titers as wild type viruses in Vero E6, MA104, and CaCo2 cells. In addition, SARS-CoV replication in airway epithelial cultures generated from Golden Syrian hamster tracheas reached similar titers to the human cultures by 72 h post-infection. Efficient SARS-CoV infection of ciliated cell-types in HAE provides a useful *in vitro* model of human lung origin to study characteristics of SARS-CoV replication and pathogenesis.

Keywords: Human airway epithelia; SARS-CoV; Coronavirus replication; SARS-CoV GFP; Coronavirus pathogenesis

1. Introduction

The importance of human coronaviruses (HCoV) as pathogens that produce severe human respiratory diseases has been greatly emphasized with the identification of the SARS-CoV and relevant model systems are needed to elucidate the underlying molecular mechanisms governing coronavirus pathogenesis and virulence in the human lung. SARS-CoV infection is an attractive model for HCoV infection as it produces severe disease in the human lung, replicates efficiently *in vitro*, reverse genetics systems are available to identify the genetic determinants governing pathogenesis and virulence, and a variety of animal models are under development (Almazan et al., 2006; Lawler et al., 2006; Martina et al., 2003; McCray et al., 2006; Osterhaus et al., 2004; Roberts et al., 2005a,b; Tseng et al., 2006; Yount et al., 2003). In this article we will provide a brief review of the pathology of SARS-CoV infection as well as

* Corresponding author. Tel.: +1 919 966 7991; fax: +1 919 966 0584.
E-mail address: sims0018@email.unc.edu (A.C. Sims).

doi:10.1016/j.virusres.2007.03.013

reviewing research examining human coronavirus infection of *in vitro* models of the human conducting airway. Finally, we will extend current data on the characterization of SARS-CoV infection of an *in vitro* culture system of human airway epithelium (HAE) that recapitulates the morphological and physiological features of the human conducting airway *in vivo* to determine whether infection and spread of SARS-CoV throughout the ciliated conducting airway may be a valid model for understanding the pathogenesis of SARS-CoV lung disease.

SARS-CoV caused about 8000 cases and ~800 deaths worldwide with a ~10% overall mortality rate prior to successful containment of the epidemic. Mortality rates following SARS-CoV infection approached <1% under 24 years of age, 6% for ages 15–44, 15% for ages 45–64 and >50% over 65, and survivors developed lung and cardiac complications (Han et al., 2003). The disease caused by this pathogenic human coronavirus is in stark contrast to that seen with other strains (229E and OC43), which produce only mild common cold symptoms, although more serious disease has been reported in infants and individuals with underlying co-morbidities (Pene et al., 2003). SARS-CoV has been isolated from humans, civet cats, raccoon dogs, swine and bats, suggesting that several animal species may function as natural reservoirs for future outbreaks (Guan et al., 2003). The Chinese horseshoe bat, which is abundant across Southeast Asia, is probably the natural reservoir for SARS-CoV (Guan et al., 2003; Lau et al., 2005; Li et al., 2005; Poon et al., 2005). Importantly, bats and bat products are used in food and traditional medicine markets in southern China and Asia and bat feces are used in traditional Chinese medicines providing a constant source of human exposure to bats and bat tissues making future SARS or SARS-like outbreaks more likely (Fujita, 1988). The SARS-CoV epidemic is the best characterized in terms of the changes that likely evolved following initial introduction of mildly virulent zoonotic strains into human populations, to moderate and highly virulent isolates that circulated around the world in less than 6 months (Chinese, 2004).

2. Clinical evidence for SARS-CoV pathogenesis

The predominant pathological features of SARS-CoV infection of the human lung include diffuse alveolar damage (DAD), atypical pneumonia with dry cough, persistent fever, progressive dyspnea and sometimes, abrupt deterioration of lung function. Major pathologic lesions include inflammatory exudation in the alveoli and interstitial tissue with hyperplasia of fibrous tissue and fibrosis. These represent major histologic changes associated with acute respiratory distress syndrome (ARDS), which has a high mortality rate and few treatment options (Cheung et al., 2004; Ksiazek et al., 2003; Kuiken et al., 2003; Nicholls and Peiris, 2005). Increasing age, male sex, presence of co-morbidity, high early viral RNA burdens, and high lactate dehydrogenase (LDH) levels are associated with greater risk of death (Chu et al., 2004; Leung and Chiu, 2004). Using fluorescence *in situ* hybridization and tissue from fatal cases of disease, virus was localized within alveolar pneumocytes (primarily type II) and within alveolar spaces. Previously, the reported receptor for SARS-CoV, the angiotensin 1 converting enzyme 2 (hACE2) had only been localized to alveolar cells in the lung although recent evidence indicates that hACE2 is present throughout the human airway epithelium suggesting additional cellular targets of infections (Jia et al., 2005). SARS-CoV specific RNA has also been localized in pulmonary macrophages although whether viable virus was present was not determined (Lu et al., 2005). In another study based on six patients who died from SARS the most pronounced morphological features were giant cell formation (predominately macrophages) and pneumocyte hyperplasia suggesting that proinflammatory cytokines released by stimulated macrophages in the alveolus were a predominant cause of pathogenesis (Nicholls et al., 2003a,b). Histological samples for determining SARS-CoV infection of airways have been less rigorously studied as pathological analyses is usually performed on late stage fatal cases (Chow et al., 2004; To et al., 2004). However, early disease noted marked bronchiolar disease with respiratory epithelial cell necrosis, loss of cilia, squamous metaplasia and intrabronchiolar fibrin deposits. In fact it has been suggested that early DAD as a result of SARS-CoV infection may initiate within the respiratory bronchioles (Franks et al., 2003; Nicholls et al., 2003a,b). It has also been hypothesized that SARS-CoV replication in the human conducting airway may be cell type restricted by expression of the receptor/co-receptor molecules hACE2 and dendritic cell-specific ICAM3-grabbing nonintegrin (DCSIGN/DCSIGNR) (Jeffers et al., 2004). DCSIGNR expression is readily detectable in alveolar type II cells the major cell type infected in the fatal cases of SARS infection. *In vitro* replication and pathogenesis models of the human conducting airway would provide a mechanism to determine all SARS coronavirus permissive cell types in the lung at earlier times post-infection and will provide clues about disease progression and potentially predict severity of disease outcome.

3. Coronavirus replication in models of the human conducting airway

3.1. SARS-CoV infection of monolayers and polarized Calu-3 cells

Several studies have been performed to identify SARS-CoV replication-competent *in vitro* models of the human conducting airway epithelium. Tseng et al. (2005) published the first SARS-CoV *in vitro* replication model using monolayers and polarized Calu-3 cells. Calu-3 cells were originally isolated from a human pulmonary adenocarcinoma and are characterized as nonciliated human lung/bronchial epithelial cells. Following inoculation of monolayers of Calu-3 cells; SARS-CoV replication was detected as early as 24 h post-infection with peak titers occurring at 48 h post-infection ($\sim 5 \times 10^6$ TCID50, Table 1). However, virus induced cytopathic effect was not detected until 8 days post-inoculation. Viral titer results were confirmed by real time PCR; with peak viral RNA detection occurring 48 h post-inoculation. Immunofluorescence assays using convalescent human serum isolated from a SARS-CoV infected patient detected SARS-CoV antigens in foci on the Calu-3 monolayers demonstrating that not all cells were productively infected. Dual labeling immunfluo-

Table 1
Respiratory virus replication in models of the human conducting airway

Virus	Cell type	Apical inoculation (AP[h])	Apical inoculation (BA[i])	Basolateral inoculation (AP)	Basolateral inoculation (BA)
SARS[a]	Calu-3 (Mono)	$\sim 5 \times 10^6$ TCID50	NA[b]	NA[b]	NA[b]
SARS[a]	Calu-3 (Diff)	$\sim 5 \times 10^7$ TCID50	2×10^2 TCID50	None	None
SARS[c]	HAE	$\sim 3.5 \times 10^4$ PFU/mL	1.3×10^1 PFU/mL	None	None
SARS[d]	HAE	$\sim 5 \times 10^6$ PFU/mL	$\sim 5 \times 10^4$ PFU/mL	None	None
229E[e]	HAE	1.05×10^4 FFU/mL	5.7×10^2 FFU/mL	9.3×10^2 FFU/mL	1×10^2 FFU/mL
RSV[f]	HAE	1×10^7 PFU/mL	None	None	None
PIV[g]	HAE	+++		–	

[a] Tseng et al. (2005).
[b] Not applicable.
[c] Jia et al. (2005).
[d] This manuscript.
[e] Wang et al. (2000).
[f] Zhang et al. (2002).
[g] Zhang et al. (2005).

rescence detected both SARS-CoV antigen and the primary viral receptor, angiotensin 1 converting enzyme 2 (hACE2), colocalized in infected Calu-3 cells suggesting that hACE2 was required for SARS-CoV entry into Calu-3 cells. To confirm that hACE2 was the primary receptor, Calu-3 monolayers were preincubated with antisera directed against hACE2 prior to inoculation. Pretreatment of cultures with antisera directed against hACE2, but not irrelevant control sera resulted in a dose dependent reduction in viral titers, suggesting that SARS-CoV was dependent on hACE2 for entry into Calu-3 cells.

To determine if SARS-CoV entry and release in Calu-3 cells were polarized, scanning confocal images of mock-infected and infected cells were taken and assembled to generate a three-dimensional image. hACE2 and SARS-CoV antigens colocalized primarily at the apical surface of the cultures, suggesting that SARS-CoV entry and release may be restricted to the apical surface of these cells. To further examine the polarity of SARS-CoV infection and release, Calu-3 cells were cultured on Transwell membranes for greater than 10 days, generating a culture of highly polarized cells connected by tight junctions and visible microvilli. Cultures were then inoculated with SARS-CoV either via the apical or basolateral surfaces and media harvested from both apical and basolateral surfaces and viral titers assayed. Inoculation of the apical surface resulted in the release of virus from both the apical (5×10^7 TCID50, Table 1) and basolateral (2×10^2 TCID50, Table 1) surfaces, although viral titers from the apical surface were four to five logs higher. Inoculation of the basolateral surface of polarized Calu-3 cells was not a productive route of infection. These studies demonstrated that SARS-CoV could productively infect bronchial epithelial cells, most likely using hACE2 as the primary receptor for entry. Virus entry and release were most productive following an apical route of inoculation suggesting a model for the release of large quantities of virus into the lumen of the lung, which could explain detection of virus in the lower airway and transmission to uninfected individuals (Table 1). However the direct relevance of these results to SARS-CoV pathogenesis in humans required a more relevant model of the human conducting airway, one that recapitulates the cell-type distribution of the human conducting airway epithelium.

3.2. 229E infection of human airway epithelial cell cultures

While the Calu-3 replication model provided clues about SARS-CoV replication in homogenous epithelial cell types, further experiments require more sophisticated models that contain multiple cell types that more faithfully represent those of the human conducting airway epithelium. The human airway epithelial cell culture system (HAE) is an *in vitro* model of the human airway epithelium. HAE recapitulate the morphological and physiological features of the human airway epithelium *in vivo* and is comprised of ciliated, non-ciliated mucin-secreting and basal epithelial cells (Pickles et al., 1998; Zhang et al., 2002). The first human coronavirus strain demonstrated to infect HAE was HCoV strain 229E (Wang et al., 2000). To provide clues for the potential routes of viral infection, HAE were first examined for the localization of the cellular receptor for 229E, CD13/aminopeptidase N that was detected exclusively at the apical surface of well-differentiated HAE suggesting that a primarily apical route of viral entry was utilized by this virus. To determine the most productive route of infection, the cultures were inoculated with 229E via both the apical and basolateral surfaces. Titers from apical surface washes were a log greater following apical, rather than basolateral inoculation demonstrating that the most productive route of inoculation and progeny virion release for 229E was via the apical surface of the epithelium (Table 1). This was the first demonstration of human coronavirus infection of the human airway epithelial cell cultures, but coronavirus infection of this model was not investigated further until the identification of the SARS-CoV in 2002.

3.3. SARS-CoV replication in human airway epithelial cell cultures

The first studies with SARS-CoV in well-differentiated HAE focused on the localization of the SARS-CoV receptor, hACE2 in this culture model and the polarity of virus entry and release (Jia et al., 2005). hACE2 was detected primarily on the apical surface of well-differentiated HAE cultures, with little to no staining detected on the basolateral surface. In contrast, undifferentiated cultures had little to no detectable

hACE2 staining and as such infection of undifferentiated cultures resulted in no productive virus replication. Receptor localization of both coronavirus strains, SARS-CoV and 229E, in the well differentiated HAE cultures favored an apical route of viral entry, suggesting that the lumenal surface of the lungs were the most likely site of viral entry following human infection. Following apical inoculation, apical release titers were $\sim 3.5 \times 10^4$ PFU/mL while basolateral titers following apical inoculation peaked at 1.3×10^1 PFU/mL (Table 1). Similar to studies performed with the less pathogenic 229E virus, inoculation of SARS-CoV onto the apical surface of the well-differentiated HAE was the most productive route of infection and also the optimal site for progeny virion release (Table 1). However, further studies were required to identify the target cell type for SARS-CoV infection and to determine if hACE2 was the primary receptor for SARS-CoV entry into the HAE or if additional co-receptor molecules were required.

4. Results

4.1. SARS-CoV growth kinetics in well-differentiated HAE cultures

To determine the rate of virion release following SARS-CoV infection, well-differentiated HAE were inoculated via the apical surface with SARS-CoV (MOI 1, strain Urbani). Apical surface washes were harvested daily for a total of 8 days post-inoculation, titered by plaque assay on Vero E6 cells and the plaque forming units per mL (PFU/mL) per day plotted (Fig. 1A). Peak titers shed from the apical surface exceeded 10^6 PFU/mL, replication titers similar to that observed in Vero E6 cell monolayers. This is in contrast to the titers obtained by Jia et al. (3.5×10^4), demonstrating that SARS-CoV replication could achieve levels detected in traditional cell monolayers. However, viral titers in the basolateral compartments were low with peak titers below 10^5 PFU/mL (Fig. 1B) again confirming that SARS-CoV entry and release of progeny virions predominately occurred from the apical surface. While titers of icSARS-CoV replication from the apical surface are consistently 10^6 and higher, we do see variation with replication levels between patient codes. All HAE cultures are allowed to mature for optimal levels of cilia on the ciliated cells, but codes that have been matured for similar lengths of time can have different levels of icSARS-CoV replication. This may reflect variations in hACE2 expression levels throughout HAE culture maturation and experiments are currently underway to determine the optimal time post-plating for hACE2 expression levels. Alternatively, virus replication may be influenced by the presence of human susceptibility alleles or by the age and health status of the donor. Viral titers increased from 12 to 24 h, peaked by 48 h, and were constant through 120 h post-inoculation. By 144 h post-inoculation, viral titers decreased by two logs and remained low through 192 h (168 and 192 h, data not shown), suggesting that HAE could no longer support productive infection, potentially reflecting the lack of new cells to infect.

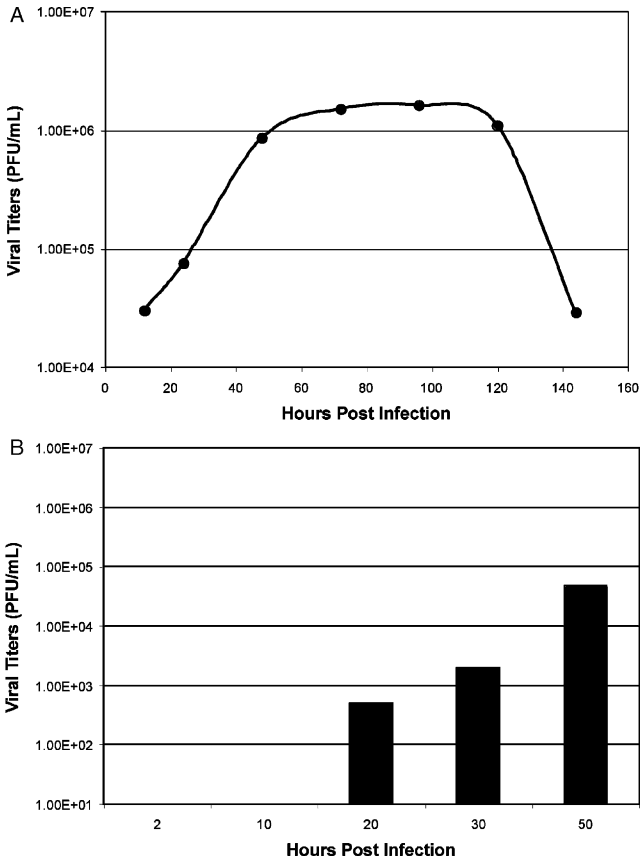

Fig. 1. Growth kinetics of icSARS-CoV in human airway epithelial cells. To determine viral growth kinetics of icSARS-CoV in HAE cultures over time, icSARS-CoV was inoculated onto the apical surface of HAE cultures and apical washes (A) and basolateral media (B) collections were performed at the indicated times. The washes were serially diluted and titers assayed on Vero E6 cells. Titers are expressed as PFU/mL.

4.2. SARS-CoV targets ciliated cells in the HAE culture system

Previous studies using the HAE model demonstrated that common human respiratory viruses, e.g. human respiratory syncytial virus (RSV) and human parainfluenza virus type 3 (PIV3) exclusively infected ciliated epithelial cell-types raising the possibility of a role of these cell-types in the pathogenesis of respiratory virus infection (Zhang et al., 2002, 2005). To determine the nature of the cell type(s) infected by SARS-CoV, transmission electron microscopy was performed on fixed cultures 48 h post-inoculation, the time point of peak viral replication in the HAE cultures. Only ciliated cell-types of the HAE inoculated with SARS-CoV contained classic coronavirus cytoplasmic vesicles filled with viral particles (Fig. 2B, E, F). In addition, large numbers of viral particles were seen within the spaces between the microvilli/cilia shafts as well as in the airway surface microenvironment (ASM) that surrounds the ciliated cells suggesting mechanisms for the release of large quantities of SARS-CoV into the lumen of the conducting airway during viral replication (Fig. 2C–F). Immuno-EM detecting the structural spike protein confirmed that the particles detected in the ASM were indeed SARS-CoV

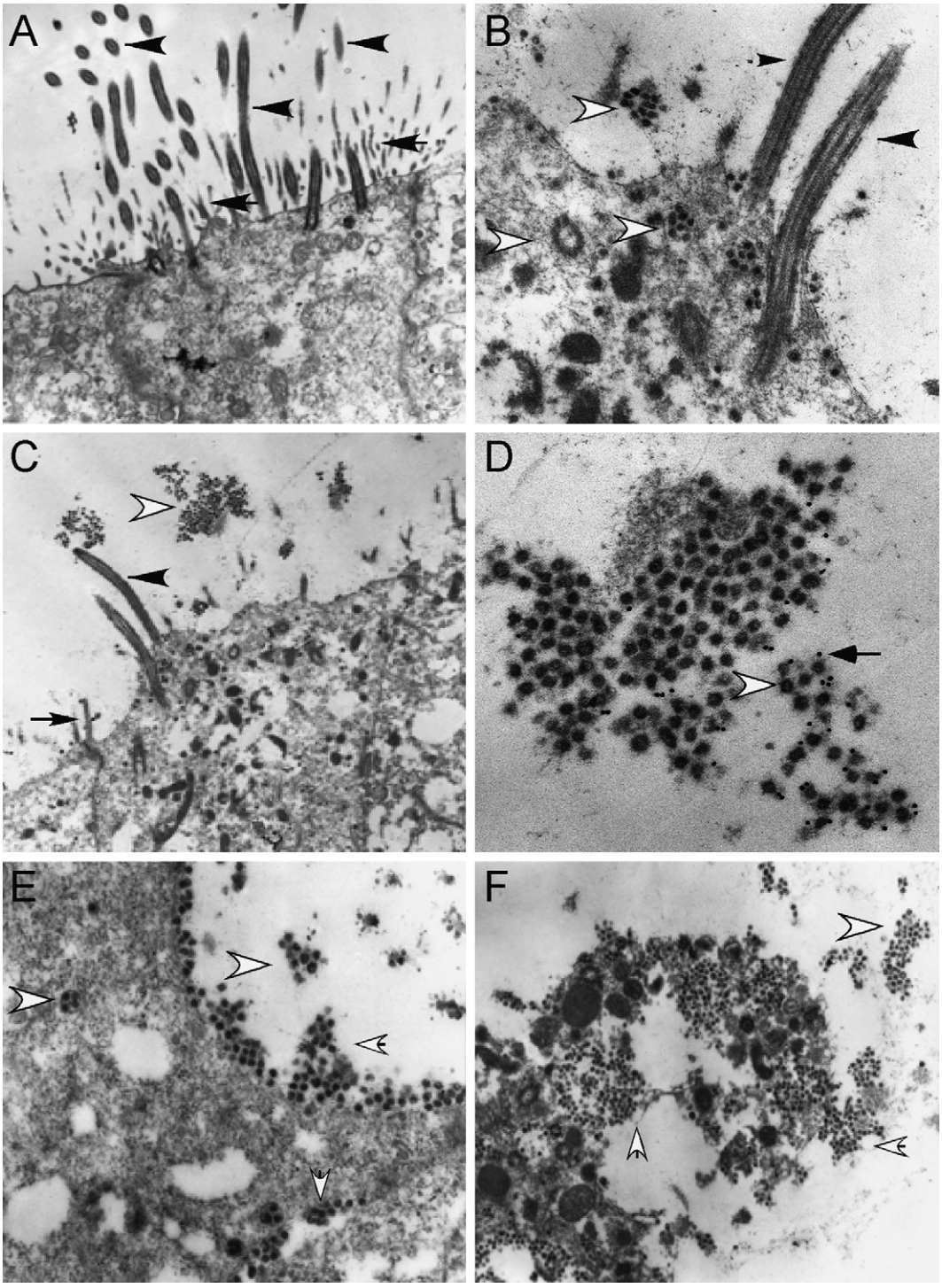

Fig. 2. Ultrastructural localization of SARS-CoV in HAE. Representative transmission electron microscopic photomicrographs of HAE infected with Urbani SARS-CoV. (A) HAE inoculated with vehicle alone demonstrating the typical morphological features of the apical surfaces of ciliated cells with prominent cilia (black arrow heads) and microvilli (arrows). (B–F) HAE inoculated with Urbani SARS-CoV 48 h before fixation and showing the presence of large numbers of virus particles (open arrow heads) in vesicles inside the ciliated cells (B and E), and on the surface of ciliated cells (B–F). To confirm the observed virions were SARS-CoV, immuno-EM was performed using polyclonal mouse antisera against S with secondary antibodies conjugated to 12 nm gold beads (D, open arrow heads indicate virions, arrows indicate colloidal gold). SARS-CoV infection resulted in extrusion and shedding of infected ciliated cells into the airway surface microenvironment (F). Similar observations were seen with HAE infected with icSARS-CoV and SARS-CoV GFP. Black arrowheads, cilia; black arrows, microvilli; open arrowhead, virions; small arrow, immuno-EM colloidal gold.

virions (Fig. 2D). Therefore, SARS-CoV entry, replication, and release occurred exclusively in the ciliated cells of the HAE.

4.3. SARS-CoV uses hACE2 exclusively to enter the ciliated cells of the HAE

Jia et al. demonstrated exclusive apical staining of the SARS-CoV receptor molecule, hACE2, using their HAE model, which is consistent with apical infection of ciliated cells. However, additional co-receptor molecules have been identified (DC-SIGN and DC-SIGNR) which might contribute to SARS-CoV entry into HAE (Jeffers et al., 2004; Marzi et al., 2004; Yang et al., 2004). To determine if SARS-CoV infects ciliated cells exclusively via an interaction with hACE2 we utilized an antibody blockade experiment using antisera directed against hACE2, a method that has previously been shown to block the interaction of SARS-CoV with hACE2 in Vero E6 cells (Li et al., 2003). HAE were pre-incubated with polyclonal or monoclonal antisera directed against hACE2 (R&D Systems), a cocktail of monoclonal antisera specific for DC-SIGN, DC-SIGNR or both, or a control antibody that efficiently binds to the apical surface of HAE (anti-tethered mucin MUC1, b27.29) for 2 h prior to inoculation with SARS-CoV (10^6 PFU/culture). Apical surface sampling was performed from 2 to 36 h post-inoculation and the samples titered by plaque assay in Vero E6 cells to determine viral growth kinetics. In the absence of antisera or in the presence of control antisera SARS-CoV replicated to titers of 10^7 PFU/mL (Fig. 3). In contrast, in the presence of hACE2 polyclonal antisera alone or in combination with other antisera, viral titers were reduced by at least two logs. Monoclonal antisera against hACE2 again failed to effect viral growth confirming that this antibody was not sufficient to block SARS-CoV entry into ciliated cells. Antisera directed against molecules reported to function as SARS-CoV coreceptors, DC-SIGN and DC-SIGNR, did not affect infection of ciliated cells by SARS-CoV although it is not known whether these antibodies sterically hinder the interaction of SARS-CoV with these potential receptors. Therefore, assessment of SARS-CoV infection by viral growth kinetics suggests that hACE2 is the predominant receptor used by SARS-CoV for infection of ciliated cell-types in HAE.

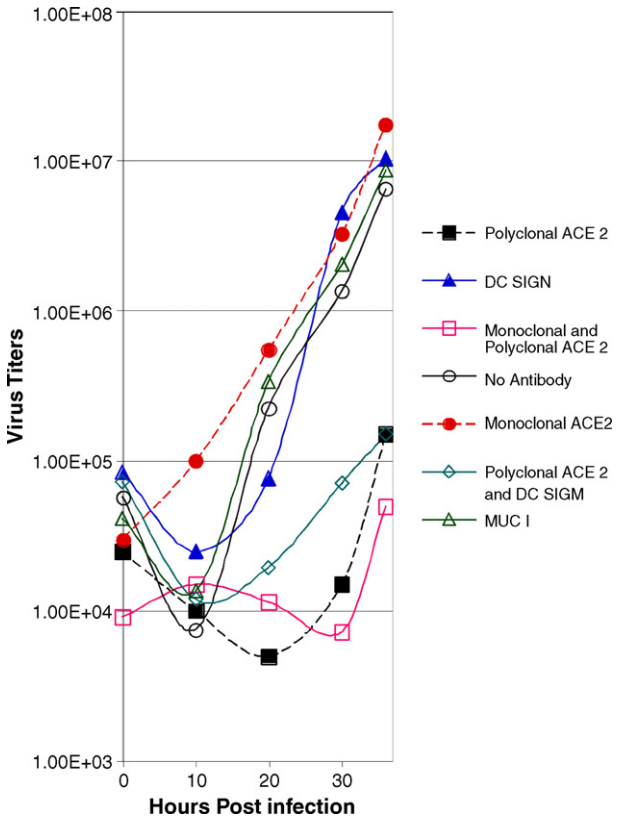

Fig. 3. hACE2 is the primary receptor for SARS-CoV entry into HAE. To assess effects of pretreatment of HAE with receptor specific antisera on the growth kinetics of SARS-CoV infection, HAE were pretreated with polyclonal or monoclonal antisera directed against hACE2 (pACE2 and mACE2, respectively), a cocktail of monoclonal antisera directed against DC-SIGN, DC-SIGNR, or both (DCSIGN), combinations of these antisera (pACE2 + DCSIGN) or an anti-MUC1 negative control antibody prior to inoculation with icSARS-CoV. Apical washes at the indicated time points were serially diluted and assayed by plaque assay on Vero E6 cells. Titers are represented by PFU/mL. Filled squares (black), polyclonal hACE2 only; filled triangles (blue), DC-SIGN/DC-SIGNR monoclonal cocktail; open square (pink), monoclonal and polyclonal hACE2; open circle (brown), no antibody; filled circle (red), monoclonal hACE2 only; open diamond (aqua), polyclonal hACE2 and DC-SIGN/DC-SIGNR monoclonal cocktail; open triangle (green), MUC 1.

4.4. SARS-CoV GFP replicates to wild type levels in three mammalian cell lines

To directly observe the extent and kinetics of SARS-CoV infection of conducting airway cultures of model animal species in real time, we constructed a recombinant SARS-CoV (SARS-CoV GFP) expressing the green fluorescent protein from the 7a/7b open reading frame. To generate recombinant SARS-CoV GFP, the F plasmid of our infectious clone was mutated to replace ORF 7a/7b with the GFP cDNA using the type IIS restriction enzyme approach described previously (Yount et al., 2002). The mutated F plasmid was confirmed by sequence analysis and amplified in *E. coli* with wild type plasmids A through E. Fragments were then isolated by digestion with the appropriate restriction enzyme, purified and ligated into a genomic length cDNA. The full-length cDNA was transcribed and genomic length RNA was co-electroporated with SARS-CoV nucleocapsid (N) transcripts into Vero E6 cells. GFP-positive cells were detected within 24 h of transfection and clarified supernatant from transfected cells when passed to fresh Vero E6 monolayers resulted in viral cytopathic effect and green fluorescent cells (Fig. 4A–C). The deletion of ORF 7a/7b did not obviously affect efficient SARS-CoV replication in tissue culture, similar to observations with TGEV and MHV when GFP was inserted into accessory ORFs of these viruses (Baric and Sims, 2005; Curtis et al., 2002; Fischer et al., 1997; Sola et al., 2003). Prior to further evaluation, five individual plaques of SARS-CoV GFP were isolated, amplified, and monitored for GFP fluorescence in addition to sequence confirmation of the mutation. All plaques contained GFP and had appropriate sequence mutations.

To evaluate the growth kinetics of SARS-CoV GFP, growth curves were generated for three different mammalian epithelial cell lines. Monolayers of Vero E6, MA104, and CaCo2 cells were inoculated with Urbani, icSARS-CoV, and SARS-

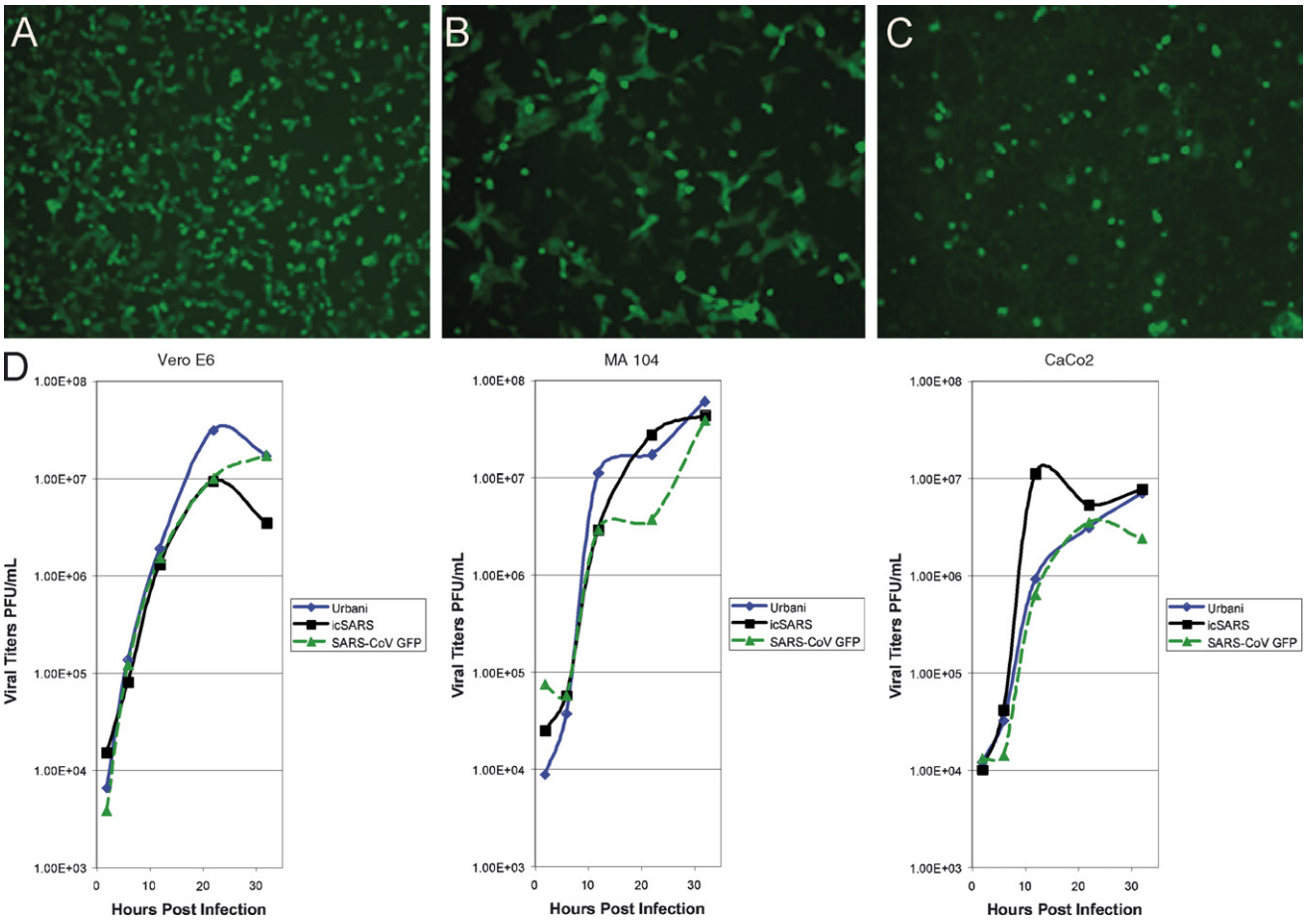

Fig. 4. Growth kinetics of Urbani, icSARS-CoV and SARS-CoV GFP in Vero E6, MA104, and CaCo2 cells. To determine viral growth kinetics of the wild type and SARS-CoV GFP viruses, three cell types were infected: (A and D) Vero E6 (African green monkey, kidney); (B and D) MA104 (African green monkey, kidney); (C and D) CaCo2 (human, colorectal adenocarcinoma). Supernatant aliquots were harvested at the indicated times post-infection, serially diluted and titers assayed on Vero E6 cells. Titers are expressed as PFU/mL. Diamonds, Urbani; squares, icSARS-CoV; triangles, SARS-CoV GFP.

CoV GFP (at an MOI 1), supernatant samples from the cultures harvested at 2, 6, 12, 22, and 32 h post-inoculation and titers determined by plaque assay on Vero E6 cells (Fig. 4D). In Vero E6 cells, Urbani and SARS-CoV GFP grew to titers of $\sim 2 \times 10^7$ PFU/mL, while icSARS-CoV peaked at $\sim 1.0 \times 10^7$ PFU/mL (Fig. 4D). For MA104 cells, all three viruses grew to titers of $(3–5) \times 10^7$ PFU/mL by 32 h post-inoculation (Fig. 4D), whereas in CaCo2 cells titers of all three viruses were reduced by approximately one log compared to MA104 cells (Fig. 4D). In addition, SARS-CoV GFP replication in HAE cultures was also similar to wild type Urbani (data not shown). Overall, replacing ORF 7a/7b with GFP in SARS-CoV GFP was not detrimental to virus replication in any of the three cell lines evaluated or HAE, thus providing a fluorescent marker of virus infection with replication at wild-type virus levels.

4.5. Susceptibility of animal airway epithelial cells to SARS-CoV infection

SARS-CoV is an emerging pathogen whose natural host, the Chinese horseshoe bat has been identified (Guan et al., 2003; Lau et al., 2005; Li et al., 2005; Poon et al., 2005). However, *in vivo* studies have shown that SARS-CoV can replicate in the mouse, hamster, cat, civet cat, ferret, and non-human primate lung (Lau and Peiris, 2005; Li et al., 2005; Martina et al., 2003; Osterhaus et al., 2004; Poon et al., 2005; Roberts et al., 2005a,b). The civet cat likely represents an important reservoir for transmission to humans (Guan et al., 2003). Airway epithelial cell cultures similar to the human model described here but derived from susceptible species may provide an important comparative model to determine the mechanisms of pathogenesis and replication efficiency in alternative hosts. Moreover, the availability of airway epithelium models from many different animal hosts may provide a method for culturing zoonotic pathogens associated with human disease outbreaks. Towards this goal we have successfully generated ciliated airway epithelium models derived from tracheobronchial airway epithelium of C57 black mice (MAE), Golden Syrian hamsters (HmAE), and rhesus macaques (RhMAE). Representative data from HmAE is shown in Fig. 5A–C. Inoculation of the apical surfaces of these cultures with SARS-CoV GFP indicated that SARS-CoV GFP replicated to some extent in ciliated cells of RhMAE, to a lesser in HmAE and to a much lesser extent in MAE, representative data from the HmAE cultures are shown Fig. 5A and B. Again, although fewer cells were infected than HAE, ciliated epithelial cell-types were the predominant cell targets

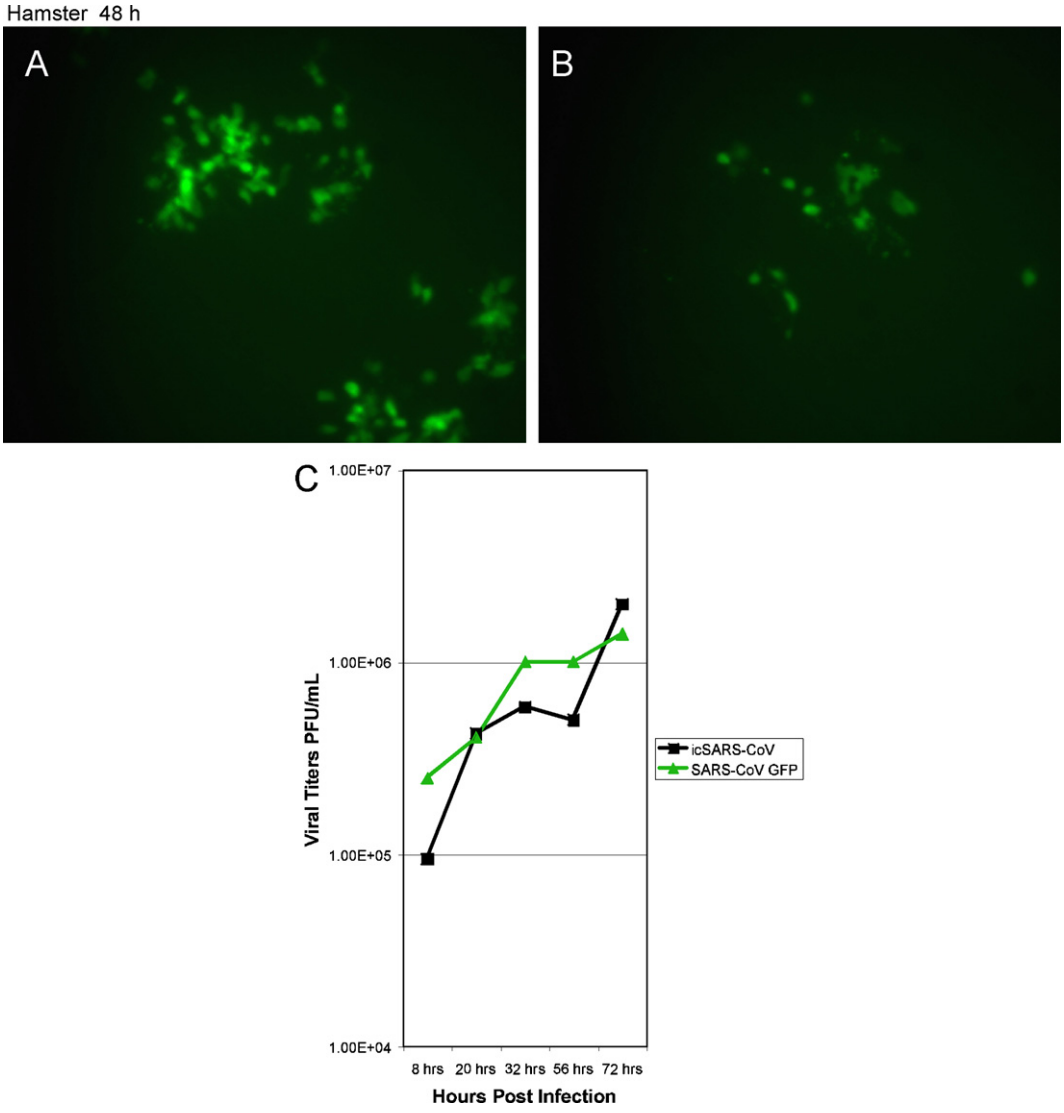

Fig. 5. SARS-CoV GFP infection of hamster airway epithelial cell cultures. (A) Ciliated airway epithelial cell cultures were derived from hamster and inoculated via the apical surface with SARS-CoV GFP (10^6 PFU). GFP fluorescent images recorded 48 h post-infection are shown. Original magnifications: 10×. (B) Growth curves for icSARS-CoV and SARS-CoV GFP in hamster cultures were obtained from apical washes collected at 0.5, 1, 2, and 3 days post-infection. Samples were serially diluted and virus tittered by plaque assay on Vero E6 monolayers. All infections were performed in triplicate. (C) Square, icSARS-CoV; triangle, SARS-CoV GFP.

for SARS-CoV GFP infection (data not shown). The growth of virus and the percentages of infected cells were greatly reduced as compared with infection rates and viral titers achieved in HAE as evidenced by growth in HmAE cultures approaching titers of $<10^6$ PFU/mL (Fig. 5C), however, a rough parallel was noted with ciliated cells derived from human > non-human primate > hamster > mouse, roughly correlating to the severity of disease noted in each species (Martina et al., 2003; McAuliffe et al., 2004; Roberts et al., 2005b; Subbarao et al., 2004; Weingartl et al., 2004). We have also observed some variation in animal epithelial culture susceptibility to infection that is dependent on the individual batch of cells used to generate the culture models; similar variation is seen in cultures derived from different human samples. Regardless, in terms of host susceptibility to SARS-CoV, HAE are the most robust airway model for studying SARS-CoV replication and pathogenesis in the lung.

5. Discussion and conclusions

The airway epithelium is often the first tissue encountered by lumenal human conducting airway pathogens and ciliated cell-types are major targets for common respiratory viruses such as RSV, PIV3 and influenza (Matrosovich et al., 2004; Thompson et al., 2006; Zhang et al., 2002, 2005) as well as SARS-CoV (Fig. 2B and C, Table 1). New emerging viruses like H5N1 also replicate efficiently in HAE cultures, providing a common airway model for comparative virus–host interactions at the site of entry into the human host (Ibricevic et al., 2006; Matrosovich et al., 2004). In our cultures, SARS-CoV replicated to high titers ($\sim 10^6$), similar to those detected in the cell line Vero E6 (Figs. 1 and 4D). Prior to infection, our HAE were cultured for a minimum of 6 weeks, allowing for maximum numbers of mature, ciliated cells which may explain

the higher titers of SARS-CoV replication. Non-polarized cultures primary human airway epithelial cells were not infected by SARS-CoV, similar to results obtained by Jia et al. (2005). Another human coronavirus, 229E, which primarily causes a mild upper respiratory tract infection in humans, has been shown to principally target ciliated epithelium, causing cell morphology alterations, dyskinesia and cilia dysfunction following HAE infection (Wang et al., 2000). However, shedding of infected ciliated cells (Fig. 2F), noted here during SARS-CoV infection, was not reported following HCoV229E infection. In contrast to other HCoV, SARS-CoV infection is associated with severe atypical pneumonia in adults. The major pathological findings on autopsy suggests SARS-CoV involvement of type II pneumocytes located in the alveoli as evidenced by detection of viral RNAs and EM detection of virus-like particles (Chen et al., 2003; Cheung et al., 2004; Zhang et al., 2003a,b). Importantly, patients dying early following SARS-CoV exposure show marked bronchiolar disease with respiratory epithelial cell necrosis, loss of cilia, squamous metaplasia and intrabronchiolar fibrin deposits. In fact it has been suggested that early diffuse alveolar damage as a consequence of SARS-CoV infection may initiate in the respiratory bronchioles (Franks et al., 2003; Nicholls et al., 2003b). The data presented support the hypothesis that SARS-CoV efficiently infects and replicates in ciliated airway cells, which concomitantly express the principle SARS-CoV receptor, hACE2. Notably, antibodies against hACE2 efficiently block infection, replication, and spread of SARS-CoV in HAE (Fig. 3) similar to results reported in Vero E6 and 293 cells expressing hACE2 (Li et al., 2003; Sui et al., 2004). Although DC-SIGN and DC-SIGNR also function as co-receptors or alternative receptors for SARS-CoV docking and entry into some cell-types (Jeffers et al., 2004; Marzi et al., 2004; Yang et al., 2004), in HAE, antibodies against DC-SIGN and DC-SIGNR did not inhibit SARS-CoV infection suggesting that these potential receptors were either less important than hACE2 for virus entry into ciliated cells or that these particular antibodies do not successfully block virus docking and entry in the presence of functional hACE2 (Fig. 3). The significant reduction of SARS-CoV infection with hACE2 antisera supports the hypothesis that hACE2 functions as the major receptor for SARS-CoV infection of ciliated cells.

By EM, large numbers of virus particles, both released from infected cells and in budding vesicles being transported to the lumenal surface were present both inside ciliated cells and in close proximity to the apical surface of ciliated cells (Fig. 2B–F). Abundant numbers of virus particles were also trapped in cellular debris in the lumenal compartment suggesting that cell-associated virus might also contribute to SARS-CoV spread between hosts. The mechanism that specifies the predominant polarized release of SARS-CoV virions is unclear, but releasing virus particles into the lumen of airways provides a means of propagating spread via interaction with potential viral receptors also polarized to the lumenal surface of ciliated cells, i.e. hACE2. Similar findings were also reported with HCoV-229E (Wang et al., 2000). As recent reports suggest that HCoV-NL63 also uses hACE2 as a receptor for entry into cells, these data indicate that many coronaviruses target this pathway while replicating in the lung epithelium (Hofmann et al., 2005). EM also demonstrated extensive cytopathology and vacuolization of infected cells, suggesting that considerable cell-associated virus may be shed from infected patients (Fig. 2F). In addition, our data demonstrate that SARS-CoV assembly and release occurs via budding into internal vesicles that are transported to the cell surface (Fig. 2B and F). Ultimately, infection results in shedding of the ciliated cell itself and these cells often contain large quantities of virus (Fig. 2F).

The HAE culture model recapitulates not only the morphological features of the human upper airway allowing visualization of the high levels of replication and destructive nature of SARS-CoV but also provides an excellent model for studying and comparing the physiological responses of the lung to a large number of respiratory virus infections. A wide range of techniques is available to determine the effect of respiratory virus infection on specific innate defense mechanisms of the airway epithelium that are recapitulated in HAE. In a well ciliated HAE culture, mucus flows over the apical surface in a continuous circular pattern due to coordinated activity of cilial beat providing an *in vitro* measure of mucociliary transport that approximates mucociliary clearance *in vivo* (Matsui et al., 1998). Fluctuations in the flow rate can be measured by observing the rotational flow of fluorescent microspheres deposited on the apical surface. Destruction and shedding of ciliated cells lead to an overall reduction in mucociliary transport, preventing the upper airway from effectively clearing viral pathogens. Another important protective component of the airway innate response to inhaled pathogens is the secretion into the airway lumen of highly glycosylated mucosubstances (e.g., MUC5AC and MUC5B) and surfactant phospholipid-protein complexes (e.g., SP-A and SP-D) (Stonebraker et al., 2004). It is predicted that different mucin species have distinct rheological/innate defense functions in the airways while their overall function is to aid in the removal of infected cells and resolve injured epithelium. The composition of the mucosubstance and surfactant production and the general levels of production of both mucins and surfactants can be used to predict disease severity with a lack of production following virus infection leading to reduced viral clearance with greater severity of disease. Immune responses to SARS-CoV can be assayed by sampling apical washes and basolateral media to measure cytokine and interferon levels as has been noted following RSV infection (Mellow et al., 2004). In addition, changes in cellular mRNA and protein levels can be determined by transcriptional and proteomic profiles, respectively.

Damage to the epithelium following infection can be monitored by determining levels of trans-epithelial resistance, a measure of the integrity of the overall epithelium, as well as levels of enzymes such as lactate dehydrogenase (LDH) that are indicators of tissue damage. It is probable that innate immune functions in the ciliated cell are critical in disease progression as these cells likely represent initial targets of infection. Innate immune responses can be monitored in the HAE cultures to determine the pathological potential for wild type and attenuated respiratory viruses in the cultures. This makes the HAE an excellent model to evaluate live attenuated respiratory virus vaccine replication and pathogenicity in the human lung prior to phase one trials. Live attenuated vaccine candidate strains

would first be assessed in human and animal airway epithelial cell cultures to determine viral growth kinetics. Low levels of replication in the culture models would be consistent with limited replication in the airway of an animal model and would indicate an inadequate vaccine candidate, prior to *in vivo* studies in animal models. HAE cultures provide a model system to study respiratory virus replication and pathogenesis, innate immune responses as well as mechanical clearance of pathogens from the human conducting airway.

Several paradigms have been proposed to explain the mechanism for spread of SARS-CoV in the human lung. One model suggests that SARS-CoV infects lung dendritic cells that transport virus to the alveolar regions allowing for infection of type II pneumocytes. This model is based on studies in which dendritic cells were infected by SARS-CoV via an interaction with over expressed levels of DC-SIGN (Marzi et al., 2004; Yang et al., 2004). An alternative model would predict that SARS-CoV infection and spread could occur through some component of the respiratory epithelium. Indeed consideration of the early pathology of SARS-CoV observed in the bronchiolar regions and the demonstration that SARS-CoV replicates efficiently in ciliated cells isolated from nasal and tracheobronchial airway regions shown here are supportive of this latter hypothesis. Moreover, the uniform gradient of hACE2 expression throughout the conducting airways of the human lung provides a suitable substrate for repeated cycles of virus amplification and spread throughout the airways, ultimately spreading to some cell component of the alveolus regions. Since specific airway epithelial cell-types especially ciliated epithelial cell-types possess unique physiological and innate defense functions in the lung it is important to determine the airway cell tropism of SARS-CoV in the human lung in order to understand the pathological consequences of infection of such cell-types.

The HAE culture systems is not only useful for examining the replication and pathogenesis of known respiratory pathogens, but can also be an excellent tool for amplifying newly identified emerging human viruses that may or may not replicate in traditional tissue culture models. The multiple cell types of the HAE culture system provide additional target cell populations for newly emerged viruses and these cultures can provide a resource for the rapid amplification of newly identified viruses for future study. Comparison studies of human versus avian influenza strains on human tracheobronchial cell cultures have demonstrated that the preferred sialic acid species for the respective virus actually reside on different cell types, which can restrict the amount of replication the avian virus can make prior to additional adaptation to the potential human host (Ibricevic et al., 2006; Matrosovich et al., 2004). Airway cultures from tracheobronchial cells from a range of animal species have also been established greatly increasing the number of viruses that can be studied, allowing the study and amplification of both zoonotic and human isolates. In addition, zoonotic viruses can be passaged on human cultures to identify mutations that arise during adaptation providing a unique look at the evolution of potential human pathogenic strains. The transition of SARS-CoV from its zoonotic origin, likely the Chinese horseshoe bat, to animals of the Chinese market place, such as the Himalayan and palm civet cat and raccoon dog, then to humans is an example of when the full potential of this model system can be utilized. We believe that HAE provide for numerous opportunities to study the pathogenesis of coronaviruses and other important human respiratory pathogens in a model reflecting much of the architecture of the human airways as well as investigating the molecular mechanisms governing virus cross-species transmission.

Acknowledgements

The authors would like to thank the Directors and team of the UNC Cystic Fibrosis Center Tissue Culture Core, the Molecular Core, and the Morphology and Morphometry Core for supplying reagents and technical expertise. In addition, we gratefully acknowledge the School of Public Health at UNC in remodeling a BSL3 facility in support of these studies. The work was supported by the National Institutes of Health through research grants AI059136, AI059443-01 and AI059443 to RSB, a University of North Carolina Medical Alumni Endowment Fund grant to RJP, and ACS was supported by Infectious Disease Pathogenesis Research Training Grant 5T32AI07151-27 through the NIH/NIAID.

References

Almazan, F., Dediego, M.L., Galan, C., Escors, D., Alvarez, E., Ortego, J., Sola, I., Zuniga, S., Alonso, S., Moreno, J.L., Nogales, A., Capiscol, C., Enjuanes, L., 2006. Construction of a severe acute respiratory syndrome coronavirus infectious cDNA clone and a replicon to study coronavirus RNA synthesis. J. Virol. 80 (21), 10900–10906.

Baric, R.S., Sims, A.C., 2005. Development of mouse hepatitis virus and SARS-CoV infectious cDNA constructs. Curr. Top. Microbiol. Immunol. 287, 229–252.

Chen, J., Zhang, H.T., Xie, Y.Q., Wan, J.W., Lu, Z.H., Wang, D.T., Wang, Q.Z., Xue, X.H., Si, W.X., Luo, Y.F., Qiu, H.M., 2003. Morphological study of severe acute respiratory syndrome (SARS). Zhonghua Bing Li Xue Za Zhi 32 (6), 516–520.

Cheung, O.Y., Chan, J.W., Ng, C.K., Koo, C.K., 2004. The spectrum of pathological changes in severe acute respiratory syndrome (SARS). Histopathology 45 (2), 119–124.

Chinese, S.M.E.C., 2004. Molecular evolution of the SARS coronavirus during the course of the SARS epidemic in China. Science 303 (5664), 1666–1669.

Chow, K.C., Hsiao, C.H., Lin, T.Y., Chen, C.L., Chiou, S.H., 2004. Detection of severe acute respiratory syndrome-associated coronavirus in pneumocytes of the lung. Am. J. Clin. Pathol. 121 (4), 574–580.

Chu, C.M., Cheng, V.C., Hung, I.F., Wong, M.M., Chan, K.H., Chan, K.S., Kao, R.Y., Poon, L.L., Wong, C.L., Guan, Y., Peiris, J.S., Yuen, K.Y., 2004. Role of lopinavir/ritonavir in the treatment of SARS: initial virological and clinical findings. Thorax 59 (3), 252–256.

Curtis, K.M., Yount, B., Baric, R.S., 2002. Heterologous gene expression from transmissible gastroenteritis virus replicon particles. J. Virol. 76 (3), 1422–1434.

Fischer, F., Stegen, C.F., Koetzner, C.A., Masters, P.S., 1997. Analysis of a recombinant mouse hepatitis virus expressing a foreign gene reveals a novel aspect of coronavirus transcription. J. Virol. 71 (7), 5148–5160.

Franks, T.J., Chong, P.Y., Chui, P., Galvin, J.R., Lourens, R.M., Reid, A.H., Selbs, E., McEvoy, C.P., Hayden, C.D., Fukuoka, J., Taubenberger, J.K., Travis, W.D., 2003. Lung pathology of severe acute respiratory syndrome (SARS): a study of 8 autopsy cases from Singapore. Hum. Pathol. 34 (8), 743–748.

Fujita, M., 1988. Flying foxes and economics. BATS 6 (Spring), 4–9.

Guan, Y., Zheng, B.J., He, Y.Q., Liu, X.L., Zhuang, Z.X., Cheung, C.L., Luo, S.W., Li, P.H., Zhang, L.J., Guan, Y.J., Butt, K.M., Wong, K.L., Chan, K.W.,

Lim, W., Shortridge, K.F., Yuen, K.Y., Peiris, J.S., Poon, L.L., 2003. Isolation and characterization of viruses related to the SARS coronavirus from animals in southern China. Science 302 (5643), 276–278.

Han, Y., Geng, H., Feng, W., Tang, X., Ou, A., Lao, Y., Xu, Y., Lin, H., Liu, H., Li, Y., 2003. A follow-up study of 69 discharged SARS patients. J. Tradit. Chin. Med. 23 (3), 214–217.

Hofmann, H., Pyrc, K., van der Hoek, L., Geier, M., Berkhout, B., Pohlmann, S., 2005. Human coronavirus NL63 employs the severe acute respiratory syndrome coronavirus receptor for cellular entry. Proc. Natl. Acad. Sci. U.S.A. 102 (22), 7988–7993.

Ibricevic, A., Pekosz, A., Walter, M.J., Newby, C., Battaile, J.T., Brown, E.G., Holtzman, M.J., Brody, S.L., 2006. Influenza virus receptor specificity and cell tropism in mouse and human airway epithelial cells. J. Virol. 80 (15), 7469–7480.

Jeffers, S.A., Tusell, S.M., Gillim-Ross, L., Hemmila, E.M., Achenbach, J.E., Babcock, G.J., Thomas Jr., W.D., Thackray, L.B., Young, M.D., Mason, R.J., Ambrosino, D.M., Wentworth, D.E., Demartini, J.C., Holmes, K.V., 2004. CD209L (L-SIGN) is a receptor for severe acute respiratory syndrome coronavirus. Proc. Natl. Acad. Sci. U.S.A. 101 (44), 15748–15753.

Jia, H.P., Look, D.C., Shi, L., Hickey, M., Pewe, L., Netland, J., Farzan, M., Wohlford-Lenane, C., Perlman, S., McCray Jr., P.B., 2005. ACE2 receptor expression and severe acute respiratory syndrome coronavirus infection depend on differentiation of human airway epithelia. J. Virol. 79 (23), 14614–14621.

Ksiazek, T.G., Erdman, D., Goldsmith, C.S., Zaki, S.R., Peret, T., Emery, S., Tong, S., Urbani, C., Comer, J.A., Lim, W., Rollin, P.E., Dowell, S.F., Ling, A.E., Humphrey, C.D., Shieh, W.J., Guarner, J., Paddock, C.D., Rota, P., Fields, B., DeRisi, J., Yang, J.Y., Cox, N., Hughes, J.M., LeDuc, J.W., Bellini, W.J., Anderson, L.J., 2003. A novel coronavirus associated with severe acute respiratory syndrome. N. Engl. J. Med. 348 (20), 1953–1966.

Kuiken, T., Fouchier, R.A., Schutten, M., Rimmelzwaan, G.F., van Amerongen, G., van Riel, D., Laman, J.D., de Jong, T., van Doornum, G., Lim, W., Ling, A.E., Chan, P.K., Tam, J.S., Zambon, M.C., Gopal, R., Drosten, C., van der Werf, S., Escriou, N., Manuguerra, J.C., Stohr, K., Peiris, J.S., Osterhaus, A.D., 2003. Newly discovered coronavirus as the primary cause of severe acute respiratory syndrome. Lancet 362 (9380), 263–270.

Lau, Y.L., Peiris, J.M., 2005. Pathogenesis of severe acute respiratory syndrome. Curr. Opin. Immunol.

Lau, S.K., Woo, P.C., Li, K.S., Huang, Y., Tsoi, H.W., Wong, B.H., Wong, S.S., Leung, S.Y., Chan, K.H., Yuen, K.Y., 2005. Severe acute respiratory syndrome coronavirus-like virus in Chinese horseshoe bats. Proc. Natl. Acad. Sci. U.S.A.

Lawler, J.V., Endy, T.P., Hensley, L.E., Garrison, A., Fritz, E.A., Lesar, M., Baric, R.S., Kulesh, D.A., Norwood, D.A., Wasieloski, L.P., Ulrich, M.P., Slezak, T.R., Vitalis, E., Huggins, J.W., Jahrling, P.B., Paragas, J., 2006. Cynomolgus macaque as an animal model for severe acute respiratory syndrome. PLoS Med. 3 (5), e149.

Leung, C.W., Chiu, W.K., 2004. Clinical picture, diagnosis, treatment and outcome of severe acute respiratory syndrome (SARS) in children. Paediatr. Respir. Rev. 5 (4), 275–288.

Li, W., Moore, M.J., Vasilieva, N., Sui, J., Wong, S.K., Berne, M.A., Somasundaran, M., Sullivan, J.L., Luzuriaga, K., Greenough, T.C., Choe, H., Farzan, M., 2003. Angiotensin-converting enzyme 2 is a functional receptor for the SARS coronavirus. Nature 426 (6965), 450–454.

Li, W., Shi, Z., Yu, M., Ren, W., Smith, C., Epstein, J.H., Wang, H., Crameri, G., Hu, Z., Zhang, H., Zhang, J., McEachern, J., Field, H., Daszak, P., Eaton, B.T., Zhang, S., Wang, L.F., 2005. Bats are natural reservoirs of SARS-like coronaviruses. Science 310 (5748), 676–679.

Lu, Y., Gong, E.C., Zhang, Q.Y., Gu, J., Li, X.W., Zhang, B., Hou, L., Shao, H.Q., Gao, Z.F., Zheng, J., Fang, W.G., Zhong, Y.F., 2005. Expression of SARS-CoV in various types of cells in lung tissues. Beijing Da Xue Xue Bao 37 (5), 453–457.

Martina, B.E., Haagmans, B.L., Kuiken, T., Fouchier, R.A., Rimmelzwaan, G.F., Van Amerongen, G., Peiris, J.S., Lim, W., Osterhaus, A.D., 2003. Virology: SARS virus infection of cats and ferrets. Nature 425 (6961), 915.

Marzi, A., Gramberg, T., Simmons, G., Moller, P., Rennekamp, A.J., Krumbiegel, M., Geier, M., Eisemann, J., Turza, N., Saunier, B., Steinkasserer, A., Becker, S., Bates, P., Hofmann, H., Pohlmann, S., 2004. DC-SIGN and DC-SIGNR interact with the glycoprotein of Marburg virus and the S protein of severe acute respiratory syndrome coronavirus. J. Virol. 78 (21), 12090–12095.

Matrosovich, M.N., Matrosovich, T.Y., Gray, T., Roberts, N.A., Klenk, H.D., 2004. Human and avian influenza viruses target different cell types in cultures of human airway epithelium. Proc. Natl. Acad. Sci. U.S.A. 101 (13), 4620–4624.

Matsui, H., Randell, S.H., Peretti, S.W., Davis, C.W., Boucher, R.C., 1998. Coordinated clearance of periciliary liquid and mucus from airway surfaces. J. Clin. Invest. 102 (6), 1125–1131.

McAuliffe, J., Vogel, L., Roberts, A., Fahle, G., Fischer, S., Shieh, W.J., Butler, E., Zaki, S., St Claire, M., Murphy, B., Subbarao, K., 2004. Replication of SARS coronavirus administered into the respiratory tract of African Green, rhesus and cynomolgus monkeys. Virology 330 (1), 8–15.

McCray, P.B., Jr., Pewe, L., Wohlford-Lenane, C., Hickey, M., Manzel, L., Shi, L., Netland, J., Jia, H.P., Halabi, C., Sigmund, C.D., Meyerholz, D.K., Kirby, P., Look, D.C., Perlman, S., 2006. Lethal infection in K18-hACE2 mice infected with SARS-CoV. J. Virol.

Mellow, T.E., Murphy, P.C., Carson, J.L., Noah, T.L., Zhang, L., Pickles, R.J., 2004. The effect of respiratory synctial virus on chemokine release by differentiated airway epithelium. Exp. Lung Res. 30 (1), 43–57.

Nicholls, J., Peiris, M., 2005. Good ACE, bad ACE do battle in lung injury, SARS. Nat. Med. 11 (8), 821–822.

Nicholls, J., Dong, X.P., Jiang, G., Peiris, M., 2003a. SARS: clinical virology and pathogenesis. Respirology 8 (Suppl.), S6–S8.

Nicholls, J.M., Poon, L.L., Lee, K.C., Ng, W.F., Lai, S.T., Leung, C.Y., Chu, C.M., Hui, P.K., Mak, K.L., Lim, W., Yan, K.W., Chan, K.H., Tsang, N.C., Guan, Y., Yuen, K.Y., Peiris, J.S., 2003b. Lung pathology of fatal severe acute respiratory syndrome. Lancet 361 (9371), 1773–1778.

Osterhaus, A.D., Fouchier, R.A., Kuiken, T., 2004. The aetiology of SARS: Koch's postulates fulfilled. Philos. Trans. R. Soc. Lond. B Biol. Sci. 359 (1447), 1081–1082.

Pene, F., Merlat, A., Vabret, A., Rozenberg, F., Buzyn, A., Dreyfus, F., Cariou, A., Freymuth, F., Lebon, P., 2003. Coronavirus 229E-related pneumonia in immunocompromised patients. Clin. Infect. Dis. 37 (7), 929–932.

Pickles, R.J., McCarty, D., Matsui, H., Hart, P.J., Randell, S.H., Boucher, R.C., 1998. Limited entry of adenovirus vectors into well-differentiated airway epithelium is responsible for inefficient gene transfer. J. Virol. 72 (7), 6014–6023.

Poon, L.L., Chu, D.K., Chan, K.H., Wong, O.K., Ellis, T.M., Leung, Y.H., Lau, S.K., Woo, P.C., Suen, K.Y., Yuen, K.Y., Guan, Y., Peiris, J.S., 2005. Identification of a novel coronavirus in bats. J. Virol. 79 (4), 2001–2009.

Roberts, A., Paddock, C., Vogel, L., Butler, E., Zaki, S., Subbarao, K., 2005a. Aged BALB/c mice as a model for increased severity of severe acute respiratory syndrome in elderly humans. J. Virol. 79 (9), 5833–5838.

Roberts, A., Vogel, L., Guarner, J., Hayes, N., Murphy, B., Zaki, S., Subbarao, K., 2005b. Severe acute respiratory syndrome coronavirus infection of golden Syrian hamsters. J. Virol. 79 (1), 503–511.

Sola, I., Alonso, S., Zuniga, S., Balasch, M., Plana-Duran, J., Enjuanes, L., 2003. Engineering the transmissible gastroenteritis virus genome as an expression vector inducing lactogenic immunity. J. Virol. 77 (7), 4357–4369.

Stonebraker, J.R., Wagner, D., Lefensty, R.W., Burns, K., Gendler, S.J., Bergelson, J.M., Boucher, R.C., O'Neal, W.K., Pickles, R.J., 2004. Glycocalyx restricts adenoviral vector access to apical receptors expressed on respiratory epithelium *in vitro* and *in vivo*: role for tethered mucins as barriers to lumenal infection. J. Virol. 78 (24), 13755–13768.

Subbarao, K., McAuliffe, J., Vogel, L., Fahle, G., Fischer, S., Tatti, K., Packard, M., Shieh, W.J., Zaki, S., Murphy, B., 2004. Prior infection and passive transfer of neutralizing antibody prevent replication of severe acute respiratory syndrome coronavirus in the respiratory tract of mice. J. Virol. 78 (7), 3572–3577.

Sui, J., Li, W., Murakami, A., Tamin, A., Matthews, L.J., Wong, S.K., Moore, M.J., Tallarico, A.S., Olurinde, M., Choe, H., Anderson, L.J., Bellini, W.J., Farzan, M., Marasco, W.A., 2004. Potent neutralization of severe acute respiratory syndrome (SARS) coronavirus by a human mAb to S1 protein that blocks receptor association. Proc. Natl. Acad. Sci. U.S.A. 101 (8), 2536–2541.

Thompson, C.I., Barclay, W.S., Zambon, M.C., Pickles, R.J., 2006. Infection of human airway epithelium by human and avian strains of influenza a virus. J. Virol. 80 (16), 8060–8068.

To, K.F., Tong, J.H., Chan, P.K., Au, F.W., Chim, S.S., Chan, K.C., Cheung, J.L., Liu, E.Y., Tse, G.M., Lo, A.W., Lo, Y.M., Ng, H.K., 2004. Tissue and cellular tropism of the coronavirus associated with severe acute respiratory syndrome: an in-situ hybridization study of fatal cases. J. Pathol. 202 (2), 157–163.

Tseng, C.T., Tseng, J., Perrone, L., Worthy, M., Popov, V., Peters, C.J., 2005. Apical entry and release of severe acute respiratory syndrome-associated coronavirus in polarized Calu-3 lung epithelial cells. J. Virol. 79 (15), 9470–9479.

Tseng, C.T., Huang, C., Newman, P., Wang, N., Narayanan, K., Watts, D.M., Makino, S., Packard, M., Zaki, S.R., Chan, T.S., Peters, C.J., 2006. SARS coronavirus infection of mice transgenic for the human angiotensin-converting enzyme 2 (hACE2) virus receptor. J. Virol.

Wang, G., Deering, C., Macke, M., Shao, J., Burns, R., Blau, D.M., Holmes, K.V., Davidson, B.L., Perlman, S., McCray Jr., P.B., 2000. Human coronavirus 229E infects polarized airway epithelia from the apical surface. J. Virol. 74 (19), 9234–9239.

Weingartl, H., Czub, M., Czub, S., Neufeld, J., Marszal, P., Gren, J., Smith, G., Jones, S., Proulx, R., Deschambault, Y., Grudeski, E., Andonov, A., He, R., Li, Y., Copps, J., Grolla, A., Dick, D., Berry, J., Ganske, S., Manning, L., Cao, J., 2004. Immunization with modified vaccinia virus Ankara-based recombinant vaccine against severe acute respiratory syndrome is associated with enhanced hepatitis in ferrets. J. Virol. 78 (22), 12672–12676.

Yang, Z.Y., Huang, Y., Ganesh, L., Leung, K., Kong, W.P., Schwartz, O., Subbarao, K., Nabel, G.J., 2004. pH-dependent entry of severe acute respiratory syndrome coronavirus is mediated by the spike glycoprotein and enhanced by dendritic cell transfer through DC-SIGN. J. Virol. 78 (11), 5642–5650.

Yount, B., Denison, M.R., Weiss, S.R., Baric, R.S., 2002. Systematic assembly of a full-length infectious cDNA of mouse hepatitis virus strain A59. J. Virol. 76 (21), 11065–11078.

Yount, B., Curtis, K.M., Fritz, E.A., Hensley, L.E., Jahrling, P.B., Prentice, E., Denison, M.R., Geisbert, T.W., Baric, R.S., 2003. Reverse genetics with a full-length infectious cDNA of severe acute respiratory syndrome coronavirus. Proc. Natl. Acad. Sci. U.S.A. 100 (22), 12995–13000.

Zhang, L., Peeples, M.E., Boucher, R.C., Collins, P.L., Pickles, R.J., 2002. Respiratory syncytial virus infection of human airway epithelial cells is polarized, specific to ciliated cells, and without obvious cytopathology. J. Virol. 76 (11), 5654–5666.

Zhang, Q.L., Ding, Y.Q., He, L., Wang, W., Zhang, J.H., Wang, H.J., Cai, J.J., Geng, J., Lu, Y.D., Luo, Y.L., 2003a. Detection of cell apoptosis in the pathological tissues of patients with SARS and its significance. Di Yi Jun Yi Da Xue Xue Bao 23 (8), 770–773.

Zhang, Q.L., Ding, Y.Q., Hou, J.L., He, L., Huang, Z.X., Wang, H.J., Cai, J.J., Zhang, J.H., Zhang, W.L., Geng, J., Li, X., Kang, W., Yang, L., Shen, H., Li, Z.G., Han, H.X., Lu, Y.D., 2003b. Detection of severe acute respiratory syndrome (SARS)-associated coronavirus RNA in autopsy tissues with in situ hybridization. Di Yi Jun Yi Da Xue Xue Bao 23 (11), 1125–1127.

Zhang, L., Bukreyev, A., Thompson, C.I., Watson, B., Peeples, M.E., Collins, P.L., Pickles, R.J., 2005. Infection of ciliated cells by human parainfluenza virus type 3 in an *in vitro* model of human airway epithelium. J. Virol. 79 (2), 1113–1124.